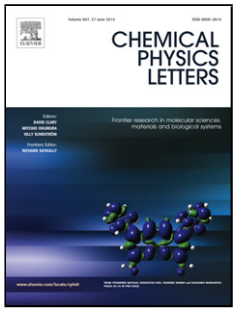

Title: Nonadiabatic photodynamics of phenol on a realistic potential energy surface by a novel multilayer Gaussian MCTDH program

Author: D. Skouteris V. Barone

PII: S0009-2614(15)00493-5
DOI: http://dx.doi.org/doi:10.1016/j.cplett.2015.06.065
Reference: CPLETT 33111

To appear in:

Received date: 24-4-2015
Revised date: 3-6-2015
Accepted date: 23-6-2015

Please cite this article as: D. Skouteris, V. Barone, Nonadiabatic photodynamics of phenol on a realistic potential energy surface by a novel multilayer Gaussian MCTDH program, *Chemical Physics Letters* (2015), http://dx.doi.org/10.1016/j.cplett.2015.06.065

- We present a calculation on the excited state dynamics of phenol.
- The calculation has been performed by a G-MCTDH algorithm written by us.
- The original surfaces are used in the calculation with no simplifications.
- An Ehrenfest-like calculation is performed on the full 33 degrees of freedom.
- The spectrum, population evolution and coordinate evolution are shown.

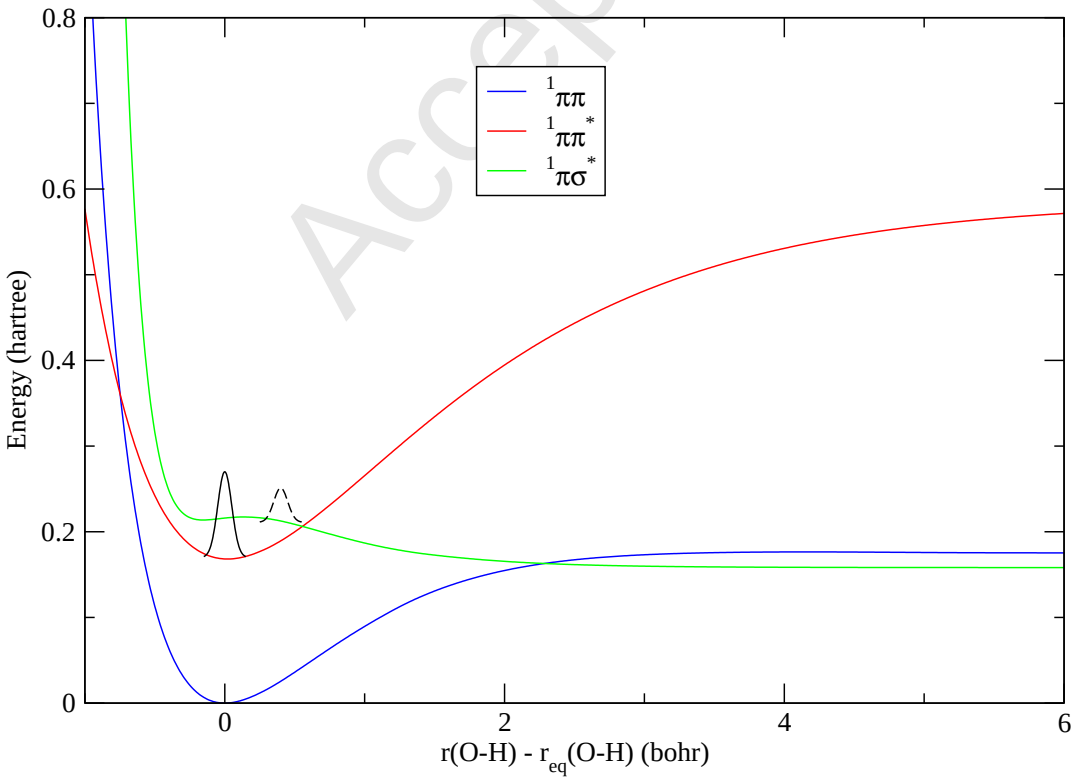

Nonadiabatic photodynamics of phenol on a realistic potential energy surface by a novel multilayer Gaussian MCTDH program

D. Skouteris*, V. Barone

Scuola Normale Superiore, Piazza dei Cavalieri 7, I-56126 Pisa, Italy

Abstract

We report the main features of a new implementation of the Gaussian Multi-Configuration Time-Dependent Hartree (G-MCTDH) model. The code allows effective computations of time-dependent phenomena, including calculation of vibronic spectra (in one or more electronic states), relative state populations etc., with the possibility of a multilayer formulation. We have validated the code on the diabatic surfaces recently published by Truhlar and coworkers to study the nonadiabatic photodynamics of phenol. Using an Ehrenfest-like, single-nuclear-configuration (but in a fully quantum formalism) model we calculate the optical spectrum and relative state populations of the system as a function of time.

Keywords: wavepacket, Gaussian, nonadiabatic, phenol

1. INTRODUCTION

Quantum dynamics is rapidly becoming an indispensable tool for studying the temporal evolution of atomic and molecular systems, from simple, elementary chemical reactions to complex biochemical and photochemical events. Up to one or two decades ago, classical mechanics represented the only tool for studying the dynamics of complex systems due to its ease of implementation and favorable scaling properties in terms of computational

*Corresponding author
Email address: dimitrios.skouteris@sns.it (D. Skouteris)

effort. However, for an accurate modelling of a process, such as might include tunnelling, quantum mechanical resonances or nonadiabatic coupling, the use of quantum dynamics is necessary.

The main drawback of quantum dynamics calculations lies in their exponential scaling with the number of degrees of freedom. One way to circumvent this problem is the use of appropriate time-dependent subspaces for the propagation of wavefunctions, as used in the multi-configuration time-dependent Hartree (MCTDH) scheme[2]. The MCTDH scheme is nowadays the method of choice for the quantum treatment of high-dimensional systems[3, 4]. Its central concept lies in the formulation of time-dependent subspaces of low dimensionality for each degree of freedom (DOF) (whose basis elements are termed single particle functions, SPFs) and the subsequent expression of the wavefunction in terms of these subspaces using also time-dependent coefficients.

The MCTDH scheme typically suffers from the necessity of a pre-fitted potential energy surface (PES) expressed as a sum of products of single-DOF terms. An alternative would be a decomposition scheme similar to MCTDH which, however, employs a time-dependent primitive basis allowing the direct use of Hamiltonian matrix elements. Such a method is provided by the Gaussian MCTDH (G-MCTDH) scheme. Gaussian functions possess a naturally localized structure which provides a classical-like picture of the evolving dynamics. Moreover, their trajectories indicate the regions of the configuration space where the potential energy is to be calculated. Gaussian wavepacket (henceforth referred to as GWP) representation was pioneered by Heller [5, 6] who made extensive use of Gaussians for various quantum dynamics problems. Sawada and Metiu [7] utilised a GWP to study curve crossing problems through a multiple trajectory theory. In 1999, Burghardt [8] and coworkers formulated the GWP representation in terms of the already successful MCTDH scheme, expressing the equations of motion as a generalization of the MCTDH ones (both within the wavefunction and the more general density matrix formalism). The first application of this method was performed by Worth and Burghardt [9] on a four-dimensional Henon-Heiles potential surface. The method was subsequently used in studying the dynamics of butadiene[10], nitrosyl chloride[11, 12], pyrazine[13] and benzene[14]. Shalashilin and Burghardt have presented a formulation of the method in terms of trajectories of coupled classical and quantum variables [15] and Mendive-Tapia et al. [16] have applied frozen-width variational Gaussian functions to study the nonadiabatic dynamics of fulvene. In general, the use

of direct dynamics with coupled Gaussian trajectories is termed the direct-dynamics variational multi-configuration Gaussian method (DD-vMCG). A review and comparison of direct dynamics methods can be found in Ref.[17]. A trajectory-guided variant of the method (coupled coherent states or CCS) has recently been compared to the standard variational Gaussian method against a number of benchmarks [18]. Within the context of direct dynamics methods, the *ab initio* multiple spawn (AIMS)[19, 20, 21] method as well as the *ab initio* multi-configuration Ehrenfest (AI-MCE)[22] and the *ab initio* multiple cloning (AIMC) method[23, 24] deserve mention. We have recently developed a general G-MCTDH code which employs the constant mean field (CMF) approach in its propagation and used it to perform calculations on the spectra of the water and glycine molecules[25].

In a recent publication, Römer and coworkers formulated a two-layer approach of the method (parallelling the highly promising multilayer MCTDH (ML-MCTDH) scheme) [26]. This method combines the G-MCTDH scheme with the contraction techniques inherent in the ML-MCTDH scheme, offering the opportunity to treat correlation between varying degrees of freedom at different levels, choosing the layer depth at which degrees of freedom are combined. We have extended our previous code into a full multilayer G-MCTDH algorithm with the possibility of admitting (in principle) an arbitrary number of layers.

In this paper we apply the new version of our code to the excited state dynamics of the phenol molecule. The photodynamics of phenol in its first two excited electronic states (S_1 and S_2) has been studied extensively, both from a theoretical and an experimental point of view. The presence of conical intersections (CI) connecting the dissociative S_2 state to both S_1 and S_0 leads to interesting dynamical features, including the possibility of tunnelling around a CI[1, 27]. Moreover, the presence of a large number of harmonic spectator modes renders it a good candidate for an effective use of the G-MCTDH scheme. The potential energy surface is used as it is, without reducing the Hamiltonian into a mathematically more tractable form. In this work, we present an Ehrenfest-like[28] calculation on all 33 vibrational degrees of freedom of the phenol molecule, taking into account the passage between different diabatic potential energy surfaces as well as their coherence. This calculation involves a single time-dependent nuclear configuration on a time-dependent linear combination of electronic states and as such cannot be regarded as a fully converged quantum calculation. The capacity of our code for a multilayer calculation will be treated in a future publication.

The paper is organized as follows. In Section 2 we present the general theory along with the relevant equations of motion as well as some specific numerical aspects of our code. In Section 3 we present some results pertaining to the photodynamics of the phenol molecule and discuss them. Section 4 concludes.

2. THEORY AND NUMERICAL DETAILS

2.1. FORMULATION

The MCTDH scheme has been amply discussed in the literature[29, 30, 31, 32] and the same is true for its multilayer version[33, 34]. The Gaussian version of MCTDH (whose original formulation can be found in Refs. [5, 6]) can be seen as an expansion of the MCTDH scheme, where the primitive functions are no longer time-independent (typically DVR) but Gaussian wavefunctions with the possibility of variationally evolving their center in phase space [8, 9, 10]. The principles of the multilayer scheme can be combined with the Gaussian formulation of MCTDH, as discussed by Römer et al.[26]. In this formulation, which is essentially the one used in our code, the overall wavefunction can be written as

$$\Psi = \sum_J A_J \Phi_J \tag{1}$$

where the A_J are complex coefficients and the Φ_J are configurations, i.e. products of single particle functions (SPFs) :

$$\Phi_J = \prod_{i=1}^{d} \phi^{(i)}_{\kappa(J,i)} \tag{2}$$

This represents the top layer expansion of the wavefunction in terms of configurations. Each of the configurations is a product of SPFs of the second highest layer. For the purposes of the present calculation, the configurations are simply products of Gaussian primitive functions. In our code, when treating multiple electronic states, both options of the single-set and the multi-set formalism are available, i.e. the electronic states can be treated as a primitive degree of freedom or, alternatively, each surface can be assigned its own network of SPFs.

The time evolution of the wavefunction is determined by the Dirac-Frenkel variational principle

$$\left\langle \delta\Psi \middle| H\Psi - i\frac{\partial\Psi}{\partial t} \right\rangle = 0 \tag{3}$$

Using this principle, the equation of motion for the coefficients is of the form:

$$i\boldsymbol{S}\dot{\boldsymbol{A}} = (\boldsymbol{H} - i\boldsymbol{\tau})\boldsymbol{A} \tag{4}$$

where $\boldsymbol{A}$ denotes the vector of coefficients. The matrices $\boldsymbol{H}, \boldsymbol{S}$ are, respectively, the Hamiltonian matrix with $H_{IJ} \equiv \langle \Phi_I \mid H \mid \Phi_J \rangle$ and the overlap matrix of configurations with $S_{IJ} \equiv \langle \Phi_I \mid \Phi_J \rangle$. The matrix $\boldsymbol{\tau}$ is the differential overlap matrix with $\tau_{IJ} \equiv \langle \Phi_I \mid \partial_t \Phi_J \rangle$ (∂_t denotes time differentiation).

The variationally evolving Gaussian parameters (expressed for the primitive particle s_k through the vector $\boldsymbol{\Lambda}^{(s_k)}$) evolve according to the equation:

$$i\boldsymbol{C}^{(s_k)}\dot{\boldsymbol{\Lambda}}^{(s_k)} = \boldsymbol{Y}^{(s_k)} \tag{5}$$

This matrix equation is of dimensionality $n_{s_k} \times p_{s_k}$, where the first factor is the number of SPFs for the primitive particle s_k and the second one is the number of physical DOF for this particle (i.e. the dimensionality of the Gaussians). The $\boldsymbol{C}$ matrix is given by

$$C^{(s_k)}_{np,n'p'} = \rho^{(s_k)}_{nn'} \langle \partial_p g^{(s_k)}_n \mid 1 - P^{(s_k)} \mid \partial_{p'} g^{(s_k)}_{n'} \rangle \tag{6}$$

where $\boldsymbol{\rho}^{(s_k)}$ and $P^{(s_k)}$ are, respectively, the density matrix and the projection operator[25].

The $\boldsymbol{Y}^{(s_k)}$ vector is given by the equation

$$Y^{(s_k)}_{np} = \sum_{n'} \langle \partial_p g^{(s_k)}_n \mid \left(1 - P^{(s_k)}\right) \tilde{H}^{(s_k)}_{nn'} \mid g^{(s_k)}_{n'} \rangle \tag{7}$$

where H stands for the mean field operator matrix[25]. It is not necessary that all or any of the primitive DOFs evolve variationally. In fact, our code takes account of the possibility of evolving the primitive SPFs along predefined trajectories or keeping them constant (as in the case of surfaces in the single-set formulation). In the latter case, the calculation is reduced to the ordinary MCTDH scheme.

Moreover, as has been previously suggested[13], we propagate, for each primitive degree of freedom, a corresponding orthonormalizing matrix $\boldsymbol{D}^{(s_k)}$ according to the equation

$$\dot{\boldsymbol{D}}^{(s_k)} = -\left(\boldsymbol{S}^{(s_k)}\right)^{-1} \boldsymbol{\tau}^{(s_k)} \boldsymbol{D}^{(s_k)} \tag{8}$$

In this way, the SPFs entering the equations of motion of higher layers are always orthonormal and the overlap and differential overlap matrices vanish from these equations.

2.2. PROPAGATION

The constant mean field scheme (CMF)[35] is used during the propagation. In accordance with this scheme, the top layer A_J coefficients are propagated linearly using the Arnoldi algorithm[36]. All other parameters (whose EOM are non-linear due to the presence of the projection operator) are propagated using a fourth order Runge-Kutta[37] scheme. In order to propagate each set of coefficients, we need:

1. The appropriate $\boldsymbol{S}$ matrices (for primitive particles this includes overlaps between derivatives of SPFs with respect to the center in phase space)
2. The appropriate $\boldsymbol{\tau}$ matrices
3. The appropriate density and mean field matrices

The first two of these items are most naturally evaluated in a "bottom-up" scheme, starting from the primitive particles and working one's way up to the top layer, and this is the method used in our program. On the other hand, for the density and mean field matrices, the most convenient scheme is a "top-down" one, starting from the top layer up to the primitive particles (the single-hole function for the top layer is simply the vacuum state). This is the method followed for the calculation of density matrices.

However, for the mean field matrices we follow a different scheme. In ordinary MCTDH calculations, the Hamiltonian is typically decomposed into a "sum of products" form. The matrix elements of individual factors in the Hamiltonian are calculated in a "bottom-up" scheme (arriving up to the Hamiltonian matrix of the top layer) and, subsequently, mean field matrix elements are calculated in a "top-down" scheme as suggested by Manthe[38]. On the other hand, the advantage of the G-MCTDH scheme lies in the possibility of performing calculations "on the fly" even when the Hamiltonian is not expressible as a sum of products. Therefore, our method of dealing with the Hamiltonian consists in the scheme:

- Express all SPFs of each particle s_k as linear combinations of products of primitive SPFs. This is most conveniently done in a "bottom-up" way.
- Express all single-hole functions of each particle s_k as linear combinations of products of primitive SPFs. This is most conveniently done in a "top-down" way.
- Loop over all pairs of combinations of primitive SPFs, obtaining the appropriate Hamiltonian matrix element and calculating its contribution to all mean field matrix elements using the coefficients calculated previously.

Note that, in this way, we retain the "bottom-up and top-down" scheme proposed by Manthe but we only use it at the coefficients level, keeping the actual Hamiltonian at the primitive level (as dictated by the G-MCTDH scheme). Obviously, the calculation will become prohibitively expensive if the number of primitive SPFs becomes too large (as in the case of ordinary MCTDH) and countermeasures have to be taken, such as expressing the Hamiltonian as a sum of products.

We use the midpoint method for the propagation, evaluating the discretisation error as the overlap between the two midpoint wavepackets generated. If a prespecified error threshold is exceeded, the time step is reduced and the step is repeated whereas if the error is well below the threshold, the time step is increased.

3. APPLICATION TO THE PHENOL MOLECULE

3.1. COMPUTATIONAL PRELIMINARIES

3.1.1. Potential energy surfaces

We have applied our code to the photodynamics of the phenol molecule. For this purpose, we have used the manifold of three diabatic surfaces constructed by Truhlar and coworkers[1]. Briefly, the system consists of the ground state of phenol (referred to as the $^1\pi\pi$ or S_0 state) of A' symmetry in the C_s point group and two excited states, the $^1\pi\pi^*$ or S_1 state (of A' symmetry) and the $^1\pi\sigma^*$ or S_2 state (of A'' symmetry). Of the two excited states S_1 is bright and bound, while S_2 is dark and dissociative. One-dimensional slices of the surfaces as a function of the O-H distance for the ground state equilibrium configuration can be seen in Fig.1.

We wish to stress that the surface is used "as it is" and it has not been subjected to the POTFIT algorithm[2] commonly used in ordinary MCTDH calculations. The only operation we perform on it is a proper (anti)symmetrization of the potential matrix elements and their derivatives with respect to reflection across the planar configuration (which was deemed necessary as some elements that should have been 0 by symmetry, such as the diabatic coupling between $^1\pi\pi^*$ and $^1\pi\sigma^*$ at coplanar configurations, turned out to have very small nonzero values). It is certainly true that the use of POTFITted (or vibronic or otherwise modeled) surfaces can lead to multiple advantages in terms of computational time. However, apart from the obvious fact that a real potential energy surface captures the dynamics of the system in a more reliable manner, its pointwise use comes as close to simulating a calculation "on the fly" as possible. The states S_1 and S_2 are coupled by a conical intersection seam and there is nonzero diabatic coupling between them at off-planar geometries. In Fig.1 it can be seen that the two cross at an O-H distance of around $2.8a_0$, while S_2 also crosses S_0 at larger O-H distances. The photodissociation of phenol proceeds through an initial excitation to the bright S_1 state, followed by passage to the dissociative S_2 one. The ground S_0 state correlates diabatically with the first excited $\tilde{A}^2B_2$ state of the phenoxyl radical while the S_2 state correlates with the ground $\tilde{X}^2B_1$ state.

3.1.2. Coordinates and wavepacket

It is our intention to monitor the coordinates of the phenoxyl radical as the wavepacket evolves on the excited $^1\pi\pi^*$ surface. Therefore, we have chosen not to use the normal coordinates of phenol in our kinetic energy expression. Rather, we have separated the 33 vibrational coordinates in two groups:

- The 30 normal coordinates of the phenoxide ion on the ground diabatic surface, with no motion of the outgoing H atom.
- The 3 coordinates involving motion of the H atom and rigid motions of the phenoxide ion.

In order to describe the ground vibrational state of phenol as adequately as possible, we diagonalised the 3×3 Hessian matrix of the second group

of coordinates at the equilibrium geometry of phenol, thus obtaining 'quasi-normal' modes describing the O-H stretch, the C-O-H bend and the C-C-O-H torsion. It is in these coordinates, as well as the 30 phenoxide normal coordinates, that the initial wavepacket is constructed and the propagation takes place. For each coordinate, a Gaussian wavepacket is assumed with a width corresponding to the harmonic frequency of the particular mode. As far as the initial state is concerned, thus, we make the implicit assumption that the normal coordinates of the phenoxide ion are very similar to the ones of phenol.

In our calculations, the wavefunction is constrained to the form

$$\mid \Psi(t)\rangle = \prod_{i=1}^{33} \mid g_i(t)\rangle \times (c_1(t) \mid 1\rangle + c_2(t) \mid 2\rangle + c_3(t) \mid 3\rangle) \tag{9}$$

i.e. a product of Gaussians (one for each of the 33 degrees of freedom) and a coherent linear combination of the three surfaces. In this form, the wavefunction is reminiscent of an Ehrenfest trajectory, being essentially described by a 33-dimensional path on an average surface. However, it should be borne in mind that it is actually a wavefunction, rather than a simple trajectory that is being propagated. Moreover, the wavefunction is found on a coherent linear combination of surfaces rather than a simple weighted average.

As the ground state of phenol is planar, it is obvious that such a wavepacket will never escape the planar configuration and thus no surface crossing can be observed. In order to observe the surface crossing dynamics, we have performed two calculations, one starting from the planar configuration and one where we have artificially introduced a displacement of 10 a.u. to the out-of-plane C-C-O-H torsional coordinate.

3.2. RESULTS

There are three kinds of results we present after our simulation: the evolution of the most important coordinates, the autocorrelation function of the wavepacket (and the optical spectrum resulting from it) and the relative surface populations.

3.2.1. Coordinate evolution

Coordinate evolution makes sense in this kind of calculation, even in a quantum mechanical context. In fact, as the nuclear wavefunction is a simple product of GWPs, it can be readily associated to a trajectory. Looking at the

time evolution, it could be readily inferred that some of the modes followed oscillating trajectories at amplitudes much higher than the others. These modes, as confirmed by the calculated spectrum (shown in the next section) are of two kinds:

- In-plane C-C-C bend
- C-O stretch

Fig.2 shows the evolution of the three modes of maximum amplitude, all of which correspond to in-plane C-C-C bending within the phenyl ring (at frequencies 545, 818 and 1017 cm^{-1} at the ground state). The other two modes evolving at a substantial amplitude (not shown) correspond to C-O stretch combined with in-plane H-C-C bending and have frequencies 1420 and 1605 cm^{-1} . Neglecting very small variations in amplitude, the behavior of all these modes is essentially harmonic. For comparison, we also show the time evolution of the active mode corresponding to the O-H bend. Here it is clear that the classical motion is far from harmonic. These two facts serve to confirm that the separation between "bath" and "active" modes is a valid one.

We can quantify the excitation of the modes if we make the assumption that they are all found in a coherent state (this assumption is corroborated by their harmonic evolution). Under this assumption, one can derive a "mean" vibrational quantum number using the expression

$$\langle n \rangle = \omega x_0^2 \tag{10}$$

where ω is the angular frequency and x_0 the amplitude of the vibration (in mass-weighted atomic units). All three vibrations shown have mean quantum numbers between 0.5 and 0.8 indicating that, even though a full vibrational excitation is not quite reached, a significant amount of action is channeled into them.

3.2.2. Autocorrelation function and spectrum

The autocorrelation function of our wavepacket is given by the well-known expression

$$\phi(t) = \langle \Psi(0) \mid \Psi(t) \rangle \tag{11}$$

and an image of it is shown in Fig.3, where the lower panel exhibits the real part of the autocorrelation function for no initial displacement, while the upper one contains the corresponding one with an initial displacement. It can be seen that, even though the amplitude envelope is similar in the two cases, it tends to be smaller for the calculation with the initial displacement. This effect is obviously due to the fact that, in the second case, the wavepacket can cross to the S_2 surface and thus enjoys more freedom of motion. The Fourier transform of the autocorrelation function yields the optical spectrum of phenol and it can be seen in Fig.4, where it has been corrected for the ground state zero-point energy. The lower and upper panels of Fig.4 correspond, respectively, to the lower and upper panels of Fig.3. The main (0-to-0) peak corresponds to an energy of 4.3 eV, in agreement with the $S_1 - S_0$ separation. At higher energies, one can observe peaks corresponding to various excited in-plane vibrational modes. As previously mentioned, and in accordance with the results obtained by Truhlar and coworkers, the main excitations correspond to C-C-C bending motions within the ring and C-O stretching (as well as overtones and combination bands).

Turning to the spectrum corresponding to the initial out-of-plane displacement, the first thing to notice is an overall blue shift of the spectrum by around 527 cm^{-1}. Bearing in mind the fact that the bath modes (such as the C-C-C bends and the C-O stretch) have very similar frequencies in both the S_1 and S_2 states, it can be guessed that this shift is due to the energy separation of the two states. Indeed, if one takes into account the relative populations of the two states (shown in the next section), this shift turns out to be of the order expected from a weighted average of the S_1 and S_2 states. Again, the C-C-C bends and the C-O stretch turn out to be the main modes excited. On the other hand, no clear line corresponding to the out-of-plane torsion is seen. We expect that the reason for this lies in the very different characteristics of this "active" mode between the two states, which causes a spreading out of its features in the spectrum.

3.2.3. Relative surface populations

In Fig.5 are shown the relative surface populations for the case when an initial out-of-plane displacement is performed on the wavepacket. It can be seen that the S_0 state is essentially never populated during the propagation due to its being energetically far away from S_1. Instead, the S_2 state is populated and the relevant population exhibits a periodic pattern, reminiscent of the well-known Rabi oscillations. Examining the evolution of the out-

of-plane torsion we have verified indeed that it varies very slowly with time, constituting essentially a constant perturbation. The period of the oscillation is around 130 atomic time units, which corresponds to an energy separation of 1.315 eV, very close to the separation between the S_1 and S_2 states in the Franck-Condon region (around 1.2 eV). Near 25000 atomic time units a minimum in the oscillation amplitude is seen. We have verified that this is due to a torsional flipping of the hydroxyl H atom to the other side of the molecular plane, which momentarily cancels the intersurface coupling.

4. CONCLUSIONS

The main advantage of quantum dynamics calculations using the MCTDH scheme (and, in particular, its G-MCTDH version) lies in the possibility of treating systems with a large number of degrees of freedom. In this, one can either split the system into a number of strongly interacting smaller subsystems (weakly interacting with each other) or else isolate the main system under study and treat the rest of the degrees of freedom as a bath (harmonic or otherwise). Both these possibilities are further facilitated by the multilayer version which allows one to base the dynamics of the system to an appropriate separation of the degrees of freedom depending on their degree of correlation.

In this work we have used our newly developed G-MCTDH code to study the nonadiabatic photodynamics of the phenol molecule, based on the surfaces calculated by Truhlar and coworkers. We have performed a calculation assigning a Gaussian wavefunction to each of the 33 degrees of freedom of phenol, coupled to a coherent linear combination of the three surfaces. We have performed two calculations based on this scheme, one starting from a Franck-Condon wavefunction on the S_1 state and one where an initial displacement of 10.0 a.u. was given to the C-C-O-H torsional mode. In the latter case, crossings to the dissociative S_2 state could be observed. The S_1 vibrational modes excited were primarily C-C-C bends and the C-O stretch, in line with the observations of Truhlar. This trend was also seen in the optical spectrum derived by the autocorrelation function.

It is clear that full convergence is not reached here. In order to achieve it, an Ehrenfest-like calculation is not enough and more Gaussians will need to be added. This is inevitably expected to render the computation more expensive, as both intra-mode representation and inter-mode correlation have to be handled in a satisfactory way. However, we expect that, with a wise

choice of Gaussian widths we can keep the number of Gaussians within a single mode to a minimum. Moreover, the correlation issue can be addressed in an optimal way by choosing an appropriate layering scheme of the degrees of freedom. On this we wish to point out that our code is in principle capable of handling any Gaussian multilayer scheme describing a molecular system and any number of Gaussians can be used in a single degree of freedom, describing the true wavefunction with arbitrary accuracy. Unfortunately, this gives rise to the common problem of Gaussians approaching each other too closely in phase space and the system becoming near-singular. Currently we are working on alleviating this problem as well as on the improvement of the efficiency of the code (in particular alternative implementations of the CMF scheme) in order to be able to handle such calculations using a minimum of computational time. Towards this end, computational tricks used in other cases as in the ab initio multiple cloning scheme[23, 24] may well prove valuable. We believe that the multilayer G-MCTDH scheme, coupled with a wise separation and layering of the degrees of freedom, can be of valuable help in elucidating the dynamics of quantum systems of high dimensionality.

5. ACKNOWLEDGMENTS

DS wishes to thank the European Research Council for a fellowship in the framework of the ERC Advanced Grant Project DREAMS "Development of a Research Environment for Advanced Modeling of Soft Matter", GA N. 320951.

References

[1] X. Xu, J. Zheng, K. R. Yang and D. G. Truhlar, Chem. Sci. **5**, 4661 (2014).

[2] M. H. Beck, A. Jäckle, G. A. Worth and H.-D. Meyer, Phys. Rep. **324**, 1 (2000).

[3] A. Raab, G. A. Worth, H.-D. Meyer and L. S. Cederbaum, J. Chem. Phys. **110**, 936 (1999).

[4] D. Skouteris and A. Laganà, Chem. Phys. Lett. **575**, 18 (2013).

[5] E. J. Heller, J. Chem. Phys. **62**, 1544 (1975).

[6] E. J. Heller, J. Chem. Phys. **75**, 2923 (1981).

[7] S. Sawada and H. Metiu, J. Chem. Phys. **84**, 227 (1986).

[8] I. Burghardt, H.-D. Meyer and L.S. Cederbaum, J. Chem. Phys. **111**, 2927 (1999).

[9] G. Worth and I. Burghardt, Chem. Phys. Lett. **368**, 502 (2003).

[10] G. A. Worth, M. A. Robb and I. Burghardt. Faraday Discuss. **127**, 307 (2004).

[11] B. Lasorne, M. J. Bearpark, M. A. Robb and G. A. Worth, Chem. Phys. Lett. **432**, 604 (2006).

[12] B. Lasorne, M. A. Robb and G. A. Worth, Phys. Chem. Chem. Phys. **9**, 3210 (2007).

[13] I. Burghardt, K. Giri and G. A. Worth, J. Chem. Phys. **129**, 174104 (2008).

[14] B. Lasorne, M. J. Bearpark, M. A. Robb and G. A. Worth, J. Phys. Chem. A **112**, 13017 (2008).

[15] D. V. Shalashilin and I. Burghardt, J. Chem. Phys. **129**, 084104 (2008).

[16] D. Mendive-Tapia, B. Lasorne, G. A. Worth, M. A. Robb and M. J. Bearpark, J. Chem. Phys. **137**, 22A548 (2012).

[17] G. A. Worth, M. A. Robb and B. Lasorne, Mol. Phys. **106**, 2077 (2008).

[18] M. Ronto and D. V. Shalashilin, J. Phys. Chem. A **117**, 6948 (2013).

[19] T. J. Martinez, M. Ben-Nun and R. D. Levine, J. Phys. Chem. **100**, 7884 (1996).

[20] M. Ben-Nun and T. J. Martinez, Adv. Chem. Phys. **121**, 439 (2002).

[21] A. M. Virshup, C. Punwong, T. V. Pogorelov, B. A. Lindquist, C. Ko and T. J. Martinez, J. Phys. Chem. B **113**, 3280 (2009).

[22] D. V. Shalashilin, J. Chem. Phys. **132**, 244111 (2010).

[23] D. V. Makhov, W. J. Glower, T. J. Martinez and D. V. Shalashilin, J. Chem. Phys. **141**, 054110 (2014).

[24] D. V. Makhov, T. J. Martinez and D. V. Shalashilin, Phys. Chem. Chem. Phys. **11**, 3316 (2015).

[25] D. Skouteris and V. Barone, J. Chem. Phys. **140**, 244104 (2014).

[26] S. Römer, M. Ruckenbauer and I. Burghardt, J. Chem. Phys. **138**, 064106 (2013).

[27] X. Xu, J. Zheng, K. R. Yang and D. G. Truhlar, J. Am. Chem. Soc. **136**, 16378 (2014).

[28] A. D. McLachlan, Mol. Phys. **64**, 839 (1964).

[29] H.-D. Meyer, U. Manthe and L. S. Cederbaum, Chem. Phys. Lett. **165**, 73 (1990).

[30] U. Manthe, H.-D. Meyer and L. S. Cederbaum, J. Chem. Phys. **97**, 3199 (1992).

[31] H.-D. Meyer, U. Manthe and L. S. Cederbaum, in *Numerical Grid Methods and their Application to Schrödinger's Equation,*edited by C. Cerjan (Kluwer Academic Publishers, Dordrecht, 1993), pp. 141-152.

[32] U. Manthe, H.-D. Meyer and L. S. Cederbaum, J. Chem. Phys. **97**, 9062 (1992).

[33] H. Wang and M. Thoss, J. Chem. Phys. **119**, 1289 (2003).

[34] O. Vendrell and H.-D. Meyer, J. Chem. Phys. **134**, 044135 (2011).

[35] M. H. Beck and H.-D. Meyer, Z. Phys. D **42**, 113 (1997).

[36] W. E. Arnoldi, Q. Appl. Math. **9**, 17 (1951).

[37] J. C. Butcher, Appl. Numer. Math. **20**, 247 (1996).

[38] U. Manthe, J. Chem. Phys. **128**, 164116 (2008).

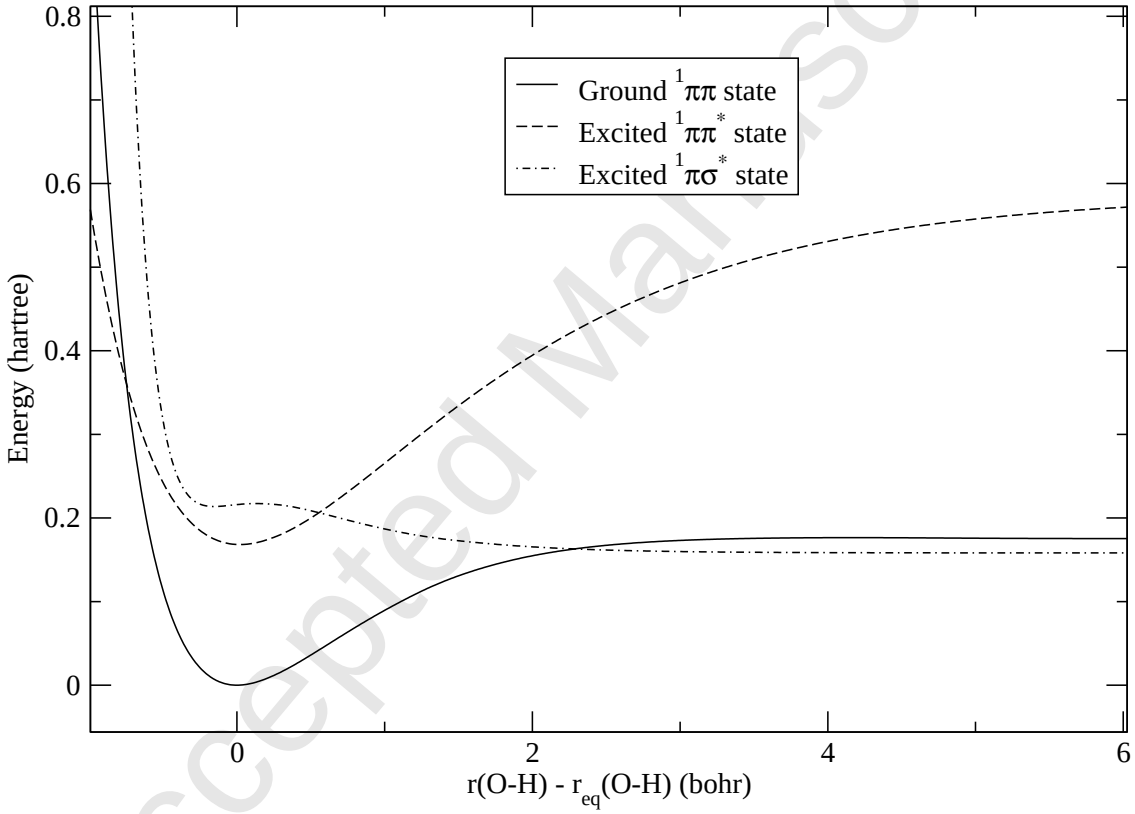

Figure 1: The three diabatic states of phenol as a function of the O-H stretching coordinate.

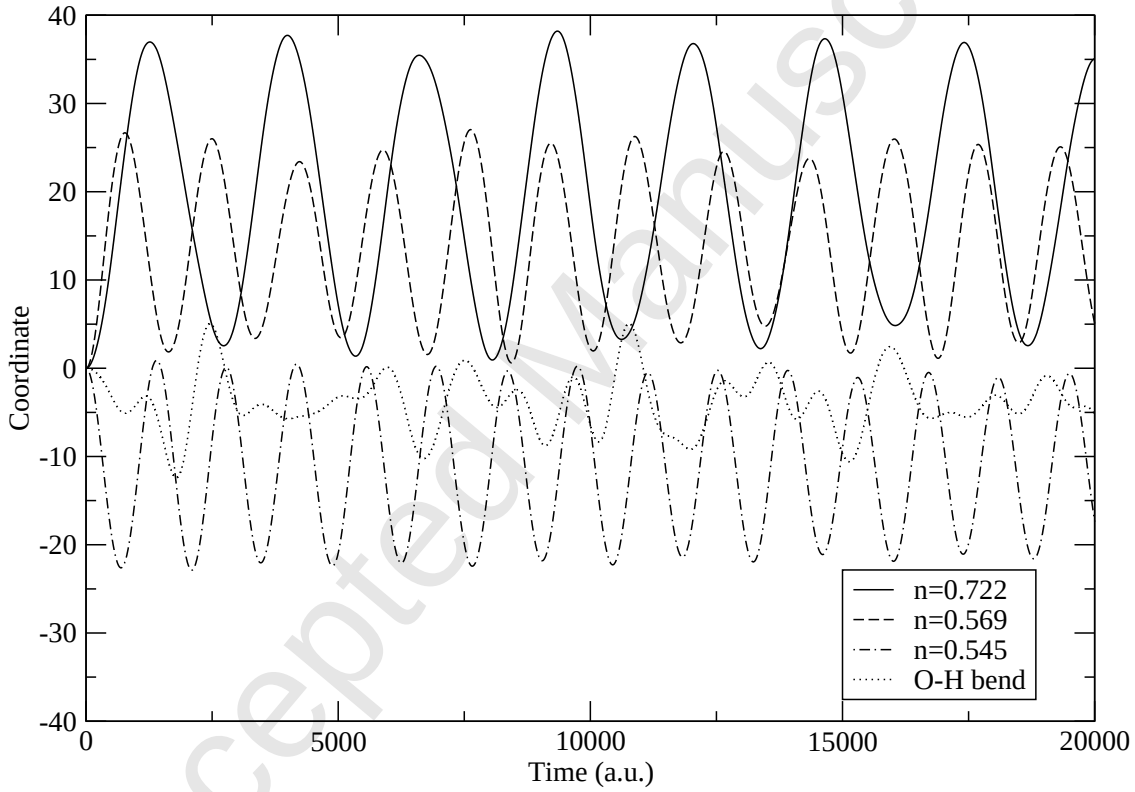

Figure 2: The three most activated background vibrations in the $^1\pi\pi^*$ state (with no initial excitation). All of them correspond to C-C-C bending vibrational modes.

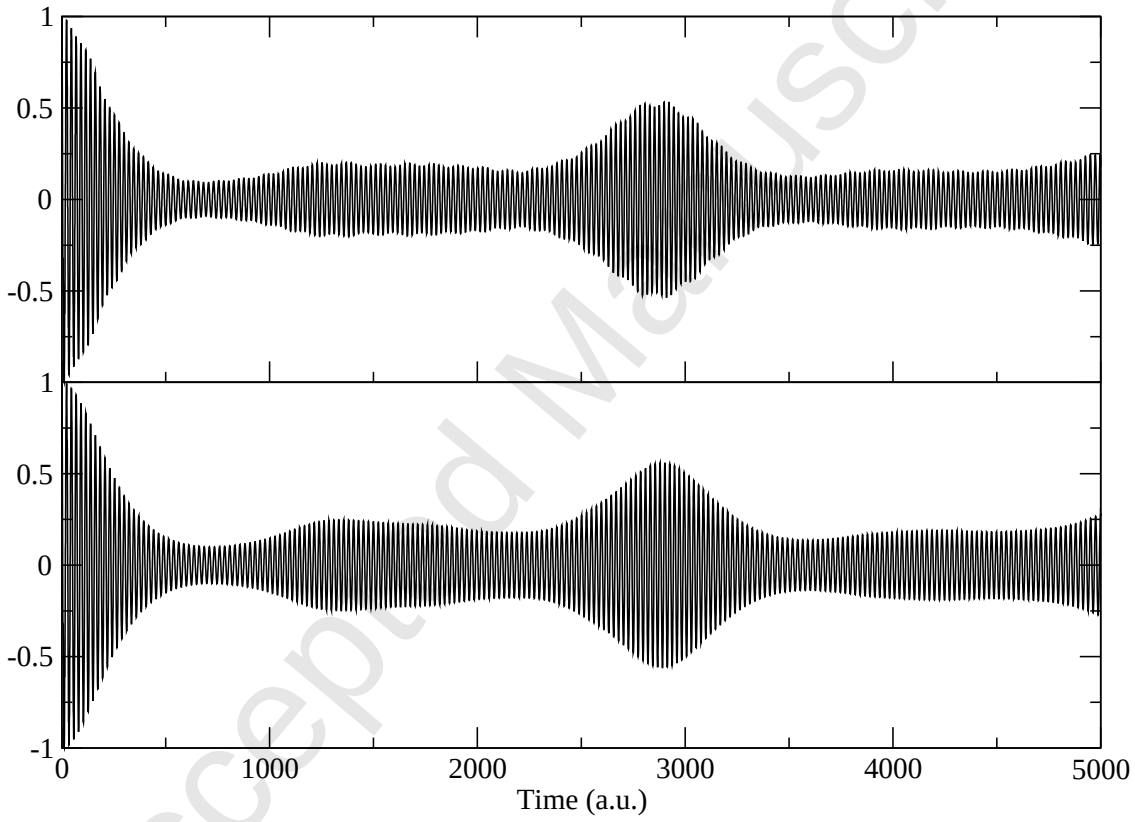

Figure 3: The real part of the autocorrelation function for no initial excitation (lower panel) and with initial excitation (upper panel).

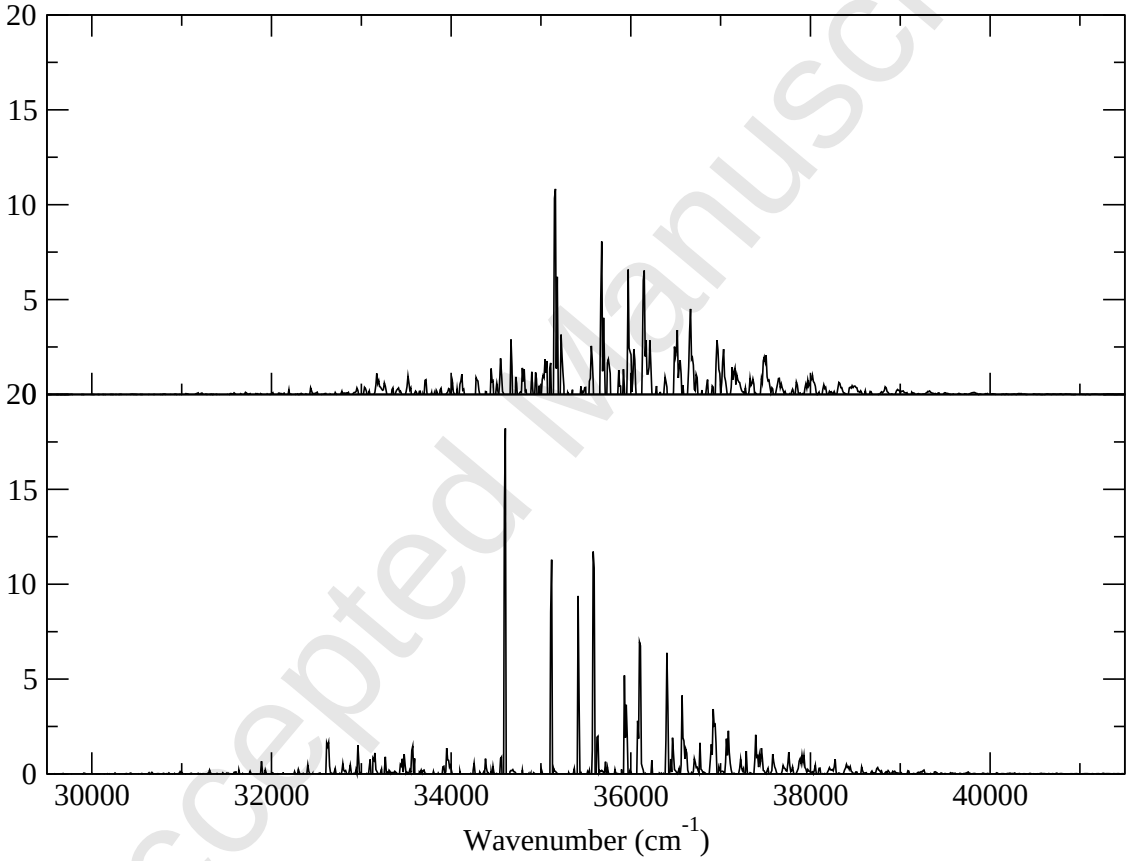

Figure 4: The excitation spectrum of phenol as calculated by an Ehrenfest-like calculation with no initial excitation (lower panel) and with initial excitation (upper panel).

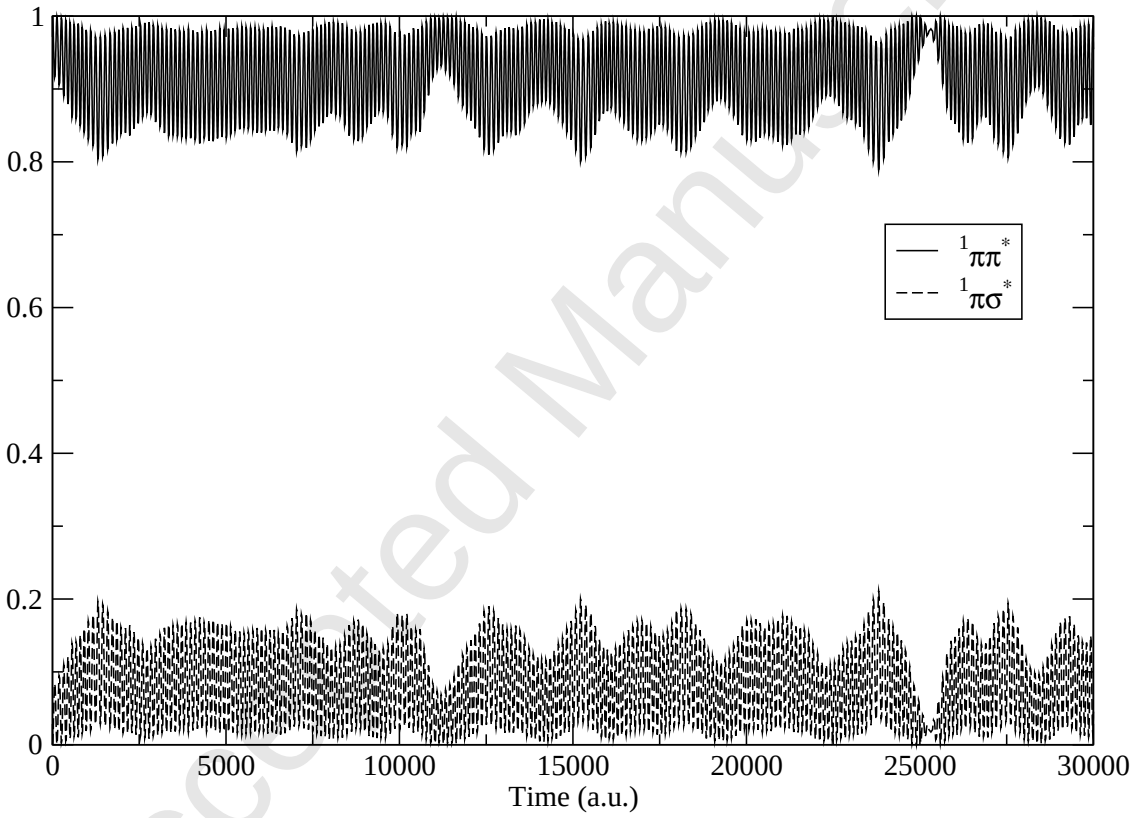

Figure 5: Time-dependent surface populations for the case of initial excitation (as diagonal elements of the density matrix).